Amino Acids (2013) 44:461–472
DOI 10.1007/s00726-012-1354-3

ORIGINAL ARTICLE

TAT-CC fusion protein depresses the oncogenicity of BCR-ABL in vitro and in vivo through interrupting its oligomerization

Zheng-Lan Huang · Miao Gao · Mao-Sheng Ji · Kun Tao · Qing Xiao · Liang Zhong · Jian-Ming Zeng · Wen-Li Feng

Received: 13 April 2012 / Accepted: 26 June 2012 / Published online: 11 July 2012

Abstract Chronic myeloid leukemia (CML) is a clonal hematologic malignancy characterized by the BCR-ABL protein. BCR-ABL is a constitutively active tyrosine kinase and plays a critical role in the pathogenesis of CML. Imatinib mesylate, a selective tyrosine kinase inhibitor, is effective in CML, but drug resistance and relapse occur. The coiled-coil (CC) domain located in $BCR_{1–72}$ mediates BCR-ABL tetramerization, which is essential for the activation of tyrosine kinase and transformation potential of BCR-ABL. CC domain is supposed to be a therapeutic target for CML. We purified a TAT-CC protein competively binding with the endogenous CC domain to reduce BCR-ABL kinase activity. We found that TAT-CC co-located and interacted with BCR-ABL in Ba/F3-p210 and K562 cells. It induced apoptosis and inhibited proliferation in these cells. It increased the sensitivity of these cells to imatinib and reduced the phosphorylation of BCR-ABL, CRKL and STAT5. We confirmed that TAT-CC could attenuate the oncogenicity of Ba/F3-p210 cells and diminish the volume of K562 solid tumor in mice. We conclude targeting the CC may provide a complementary therapy to inhibit BCR-ABL oncogenicity.

Z.-L. Huang and M. Gao contributed equally to this work.

Z.-L. Huang · M. Gao · M.-S. Ji · K. Tao · L. Zhong · J.-M. Zeng · W.-L. Feng (✉)
Department of Clinical Hematology, Key Laboratory of Laboratory Medical Diagnostics Designated by the Ministry of Education, Chongqing Medical University, Chongqing 400016, People's Republic of China
e-mail: fengwlcqmu@sina.com

Q. Xiao
Department of Hematology, The First Affiliated Hospital, Chongqing Medical University, Chongqing 400016, People's Republic of China

Keywords TAT · Coiled-coil domain · BCR-ABL · Oligomerization · Oncogenicity

Introduction

Chronic myeloid leukemia (CML) is a clonal hematologic malignancy characterized by the Philadelphia chromosome, which generates from the translocation between chromosome 9 and 22, t(9:22) (q34,q11) (Deininger et al. 2000; Faderl et al. 1999). The translocation forms BCR-ABL fusion gene, which codes BCR-ABL protein. BCR-ABL is a constitutively active tyrosine kinase and plays a critical role in the pathogenesis of CML (Lugo et al. 1990; Martin and James 2003; Melo and Deininger 2004). Imatinib mesylate (IM) is a selective inhibitor of the BCR-ABL tyrosine kinase (Deininger et al. 2005). The introduction of imatinib has dramatically improved the long-term prospects for survival of CML patients and it has become the front-line therapy (Baccarani et al. 2009; Druker et al. 2006; Palandri et al. 2008). However, there are more than one-third of patients who may still need alternative therapies due to intolerance or resistance to imatinib (de Lavallade et al. 2008; Volpe et al. 2009).

The primary conformation of BCR-ABL is a tetramer. The CC domain located in $BCR_{1–72}$ mediates two BCR-ABL monomers into a dimer, then two dimers stack onto each other to form a tetramer (Zhao et al. 2002). It is reported that the tetramerization of BCR-ABL is essential for its transformation and required for the ABL-kinase activation. Deletion of CC domain absolutely abrogates the transformation ability of BCR-ABL and thus fails to induce myeloproliferative diseases (MPD) in mice (McWhirter et al. 1993; Zhang et al. 2001). Therefore, disrupting BCR-ABL oligomerization represents a potential therapeutic strategy for inhibiting BCR-ABL oncogenicity (Beissert

et al. 2003). Targeting the CC domain to force BCR-ABL into a monomeric conformation may reduce BCR-ABL kinase activity and increase the sensitivity of BCR-ABL cells to imatinib. Mian and Beissert have already used retroviral system to transfect coiled-coil domain to inhibit BCR-ABL activity (Beissert et al. 2008; Mian et al. 2009). However, there are biosafety problems by using retroviruses for gene therapy. Hence, an alternative non-viral method to efficiently introduce coiled-coil domain is under our consideration.

Protein transduction domains (PTDs) which are attractive drug delivery systems have the ability to efficiently traverse cellular membranes, either alone or in association with molecular cargo (Kinyanjui and Fixman 2008). TAT delivery system is one of the PTDs, which is widely used for the delivery of macromolecules into cells in vitro and in vivo. TAT is an 11 amino acid peptide rich with arginine and lysine (Frankel and Pabo 1988; Green and Loewenstein 1988; Herce and Garcia 2007). It is well established that TAT can carry the protein fused to it to traverse cell membrane efficiently and rapidly, while maintaining their biological activity (Vive's et al. 1997). The therapeutic application of TAT delivery system seems to be unlimited (Rapoport and Lorberboum-Galski 2009). Therefore, we purified a recombinant protein TAT-CC, in which TAT can take the exogenous CC domain into cells and the latter competively bind to the endogenous CC domain of BCR-ABL and interrupt its homotetramerization. Our previous results demonstrated that TAT-CC can transduce into and locate in the cytoplasm of BCR-ABL positive and negative cells, and specifically inhibit growth and induce apoptosis in BCR-ABL positive cells, whereas, not affect BCR-ABL negative cells (Huang et al. 2011).

In the present study, we further explored the detailed mechanisms of the anti-proliferative and pro-apoptotic activity effect of TAT-CC on BCR-ABL positive cells in vitro and in vivo. Understanding these mechanisms may provide important clues to more effective CML targeting treatments.

Materials and methods

Cell culture, reagents and antibodies

Ba/F3-p210 and K562 cells were maintained in RPMI 1640 medium supplemented with 10 % fetal calf serum (Gibco, USA). Imatinib mesylate (Novartis, China) was dissolved in DMSO. Bax, Bcl-2, c-Myc and CyclinD1 antibodies were obtained from Santa Cruz Biotechnology. HA, c-Abl, phospho-c-Abl (Tyr245), phospho-Stat5 (Tyr694), phospho-CrkL (Tyr207) and eIF4E antibodies were obtained from Cell Signaling Technology, USA.

The generation of TAT-CC fusion protein

We constructed a bacterial expression vector, pTAT-CC, to produce in-frame TAT-CC fusion protein. pTAT-CC vector was constituted by an N-terminal 6-histidine leader followed by the 11-amino acid TAT protein, the coded sequence of BCR CC domain, and a hemaglutinin (HA) tag. The 6-histidine motif facilitated the purification of proteins using metal affinity chromatography. The fused CC protein competively bound with the endogenous CC domain of BCR-ABL oncoprotein to form heterogenous dimer. The HA epitope tag was convenient for immunological analysis. The TAT-CC fusion protein was purified with Ni^{+}-NTA resin (Huang et al. 2011).

Confocal laser scanning fluorescence microscope assay

60 μmol/L TAT-CC was added to exponentially growing cells for 6 h. Cells were fixed in methanol, permeabilized in 0.05 % Triton, incubated with primary antibody then secondary antibody. Cell nuclei were stained with DAPI (4′,6-diamidino-2-phenylindole). The glass slides were observed with confocal laser scanning microscopy.

Coimmunoprecipitation, pull-down assay and western blot

For coimmunoprecipitation assay, Ba/F3-p210 and K562 cells were treated with 60 μmol/L TAT-CC for 6 h then collected. The cell pellet was washed twice, incubated with trypsin (1 mg/mL) at 37 °C for 15 min to remove cellular membrane sticking TAT-CC (Richard et al. 2003), then washed twice more with cold PBS. The procedure was performed according to the kit instruction (PIERCE, ProFound™ HA Tag IP/Co-IP Kit, Product No. 23610). The elution samples were resolved by electrophoresis through 6–15 % gradient sodium dodecyl sulfate polyacrylamide gels. For pull-down assay, Ba/F3-p210 and K562 cells were collected and lysed. 25 μg of TAT-CC was added to 500 μg of Ba/F3-p210 or K562 cell lysate. After incubated at 4 °C for 6 h with end-over-end mixing, the following procedures were the same as coimmunoprecipitation. Western blot experiments have been described in detail previously (Jacquel et al. 2005). Antibody complexes were detected using the Immobilon Western Chemiluminescent HRP Substrate (Millipore, USA). Chemiluminescent bands were visualized on cool image workstation (Viagene, USA). The densitometry analysis of the western blots was measured by the Quantity One software.

Apoptotic and cell cycle analysis by flow cytometry

Cells were respectively treated with PBS, 40 μmol/L CC or 40 μmol/L TAT-CC protein for 48 h. For apoptotic

analysis, cells were stained with the combination of AnnexinV-FITC and propidium iodide (PI) or AnnexinV-PE and 7-AAD (KeyGenBiotech, China) according to the manufacturer's instructions. For cell cycle analysis, cells were fixed with 70 % ice cold ethanol then incubated in staining solution. Cell cycle phase distribution was monitored by a Beckman/Coulter EPICS Elite flow cytometer, as described previously (Schroering et al. 2009). These experiments were repeated three times.

DNA ladder assay

Cells were treated with PBS, 40 μmol/L CC or 40 μmol/L TAT-CC for 48 h. DNA fragments were extracted with Apoptotic DNA Ladder Detection Kit (Biomed, China) according to the manufacturer's instructions. The extracted DNA was electrophoresed on 1.5 % agarose gel then observed through the Thermo Gel Doc 1,000 gel image analysis system.

Ultrastructural analysis

Cells were treated with 40 μmol/L TAT-CC or PBS for 48 h. The cell pellets were fixed in 2.5 % glutaraldehyde. The following preparation was according to previous description (Strecker et al. 1993). The samples were examined and observed under a HITACHI-600 transmission electron microscope (TEM). The K562 solid tumor was sectioned into about 1 mm^3, and then prepared as cell samples.

Reverse transcription-Polymerase chain reaction (RT-PCR)

RNA was isolated from cells with RNAiso Plus according to the manufacturer's instructions (TaKaRa, China). The concentration of RNA was measured by the absorption at 260 nm with a GENE Quant pro nuclear and protein analysis system. The RNA quality was measured by electrophoresis on 1.0 % agarose gel. The reaction buffer of reverse transcription (RT) was prepared according to the manufacturer's instructions (TaKaRa, China). The RT reaction was performed at 37 °C for 15 min then 85 °C for 5 s. The cDNA was immediately used as the PCR template or stored at −20 °C. The PCR reaction buffer was prepared according to the manufacturer's instructions (TaKaRa, China). The PCR product was analyzed by electrophoresis on 2 % agarose gel. The semiquantification analysis of PCR products was made with the Quantity One analysis software.

MTT assay

Cells in exponential phase were plated in 96-well plates (1×10^3/well) and treated with PBS or 40 μmol/L CC or 40 μmol/L TAT-CC for 1–5 days, three duplications for each group. After incubation for the indicated times, 20 μL MTT solution (5 mg/mL, Sigma, USA) was added to each well and incubated for 4 h, then 100 μL DMSO was added. The absorbance was measured at 490 nm by a Tecan Infinite F200/M200 microplate reader (TECAN, Switzerland).

Wright's stain and hematoxylin–eosin staining

Cells were pelleted and smeared onto slides. Once dried, Wright's staining solution A (Baso, China) was added then solution B. Slides were observed with optical microscope. Paraffin sections were cut as 4 μm thick and dewaxed in xylene, dehydrated in descending alcohol series, and stained using a routine hematoxylin–eosin staining technique as described previously (Tzoracoleftherakis et al. 2010).

Animal studies

Studies involving animal subjects were approved by the Animal Use and Care Committee of Chongqing Medical University and conducted strictly in accordance with relevant protocols. The animal care was in accordance with institution guidelines.

Murine BCR/ABL leukemogenesis assay

Ba/F3-p210 cells were treated with PBS or 40 μmol/L TAT-CC protein for 48 h, collected and injected intravenously (1×10^6 cells) into BALB/c mice between 3 and 4 weeks as previous description ($n = 10$) (Ilaria and Van Etten 1995). Injected mice were subsequently evaluated on a daily basis for weight loss, failure to thrive, splenomegaly, or hind-limb paralysis. Mice that appeared pre-morbid were killed. Hind-limb paralysis was scored, if mice exhibited an inability to use hind limbs for ambulation on a smooth surface such as a countertop.

K562 subcutaneous solid tumor assay

1×10^7 K562 cells were subcutaneously injected into BALB/c nude mice as previous description (Gao et al. 2004). Normal BALB/c nude mice were set as control, named group a. One week later, tumors grew subcutaneously in BALB/c nude mice. These mice were divided into two groups, named group b and c. PBS was injected into tumors grown in group b mice. TAT-CC fusion protein (20 mg/mL, 0.2 mL) was injected into tumors grown in group c mice ($n = 5$). The injection was taken twice a week and went on for 3 weeks. Then tumors were removed. The weights of mice and volumes of tumors were recorded every 5 days.

White blood cell (WBC) count

Peripheral blood was obtained by cutting mouse tail. 20 μL of peripheral blood was obtained and diluted in 380 μL of

2 % glacial acetic acid. 10 μL of diluted cell solution was pooled into Neubauer hemacytometer. Cells were counted with an Eclipse 80i microscope (Nikon, Japan).

TUNEL test

Apoptosis in K562 solid tumor tissues was detected by FITC labeling of DNA strand breaks using TUNEL test, which was conducted according to the manufacturer's instructions (Roche, USA). Photomicrographs were taken with an Eclipse 80i microscope (Nikon, Japan).

Immunohistochemistry

Sections were dewaxed in xylene, re-hydrated in descending alcohol series, and unmasked antigens in citrate buffer then kept in 3 % H_2O_2. After blocking, sections were incubated with primary antibodies then secondary antibody. The resulting signal was developed with diaminobenzidine. Photomicrographs were taken with an Eclipse 80i microscope (Nikon, Japan).

Statistical analysis

Results are expressed as the mean ± SD. Statistical analysis was performed using Student's t test with $P < 0.05$ deemed as statistically significant. Kaplan–Meier survival curves were constructed using SPSS 13.0.

Results

TAT-CC fusion protein co-locates and interacts with BCR-ABL

We selected BCR-ABL positive Ba/F3-p210 and K562 cell lines as our experimental objects. Ba/F3-p210 cells are a clone of stable transfected cells generated from Ba/F3 cells transfected with $p210^{BCR-ABL}$ (Ghaffari et al. 1999). The K562 cell line derives from a CML patient in blast crisis (Klein et al. 1976). Ba/F3-p210 and K562 cells are widely used in the study of CML. TAT-CC protein was added to the cultures of Ba/F3-p210 or K562 cells. The co-location of TAT-CC and BCR-ABL was detected by confocal laser scanning fluorescence microscope (Fig. 1a). TAT-CC was detected by anti-HA primary antibody then visualized by FITC-conjugated secondary antibody. BCR-ABL was detected by anti-c-Abl primary antibody then visualized by PE-conjugated secondary antibody. Results showed that TAT-CC located in the cytoplasm of Ba/F3-p210 and K562 cells and it co-located with BCR-ABL. TAT-CC was dialyzed in PBS. Therefore, PBS group was set as solvent control. CC protein treated group was set as control to eliminate the unspecific effect brought by uncorrelated protein. We could not detect green fluorescence in PBS or CC treated cells (data not shown). We performed pull-down assay to detect if TAT-CC could pull-down BCR-ABL. TAT-CC was added to the cell lysate of Ba/F3-p210 or K562 which contains BCR-ABL protein and incubated

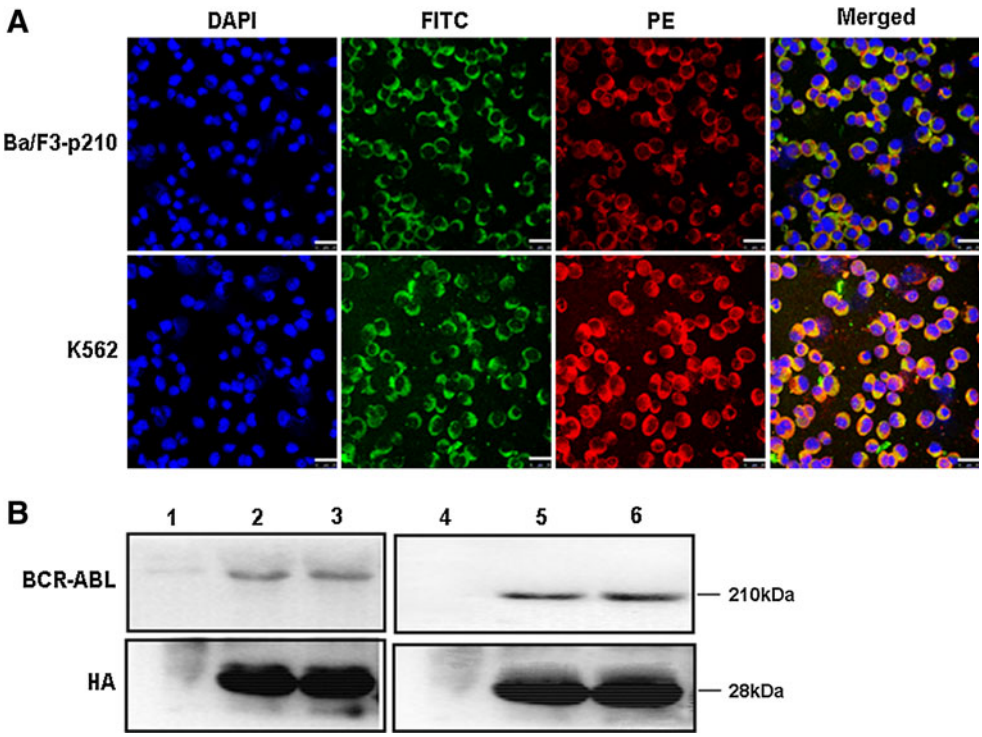

Fig. 1 TAT-CC fusion protein co-locates and interacts with BCR-ABL. Ba/F3-p210 and K562 cells were treated with 60 μmol/L TAT-CC for 6 h. **a** The location of TAT-CC and BCR-ABL was detected by confocal laser scanning fluorescence microscope. TAT-CC was visualized by FITC-conjugated secondary antibody. BCR-ABL was visualized by PE-conjugated secondary antibody. The Pixel time was 1.6 μs. The stack size was 1,024 × 1,024. Bar = 25 μm. **b** The interaction between TAT-CC and BCR-ABL. *Lanes* 1–3: Ba/F3-p210 cells. *Lanes* 4–6: K562 cells. *Lanes* 1, 4: lysate of Ba/F3-p210 and K562 cells. *Lanes* 2, 5: TAT-CC pull-downs BCR-ABL protein from cell lysate. *Lanes* 3, 6: coimmunoprecipitation assay

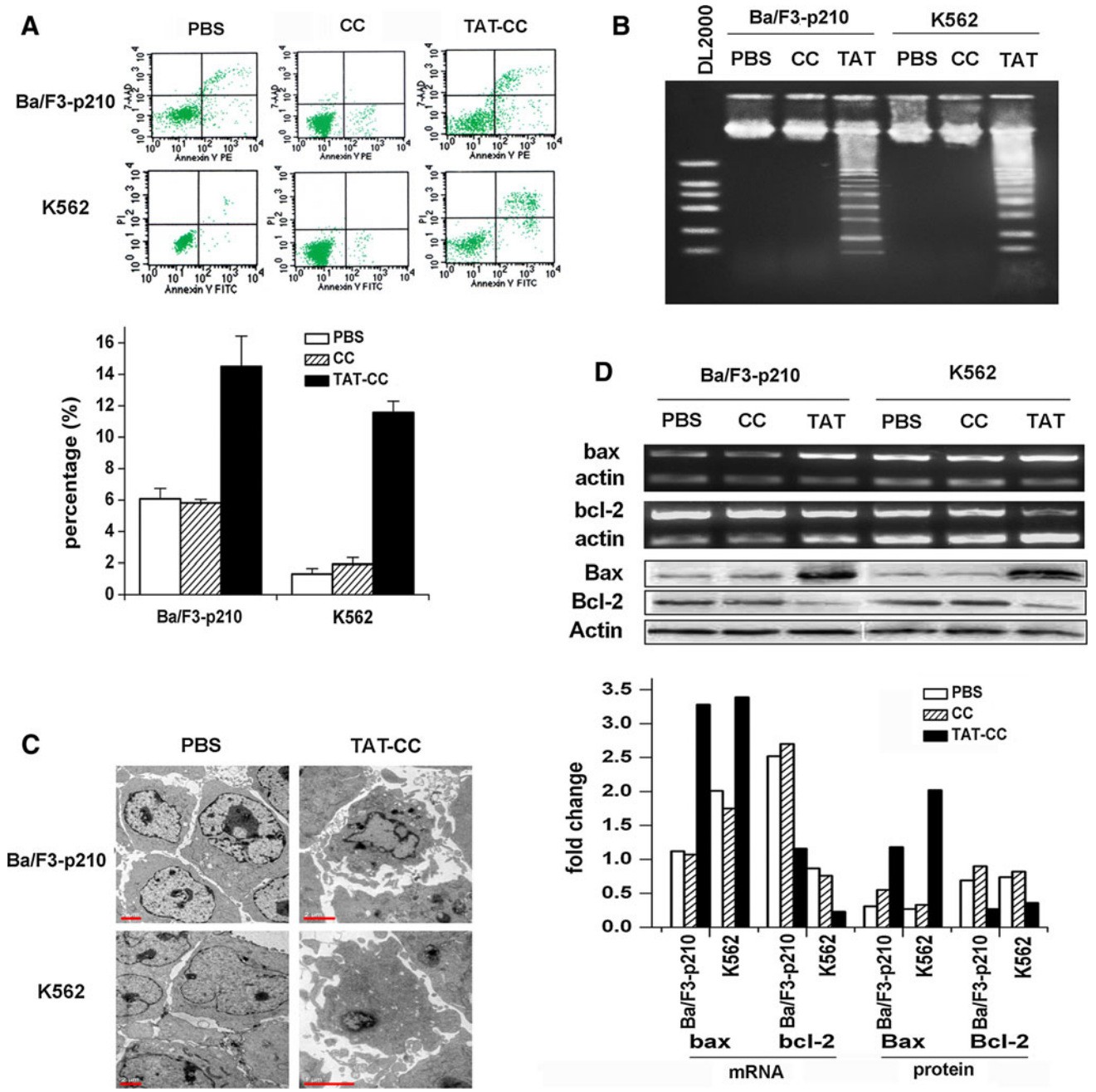

Fig. 2 TAT-CC fusion protein induces apoptosis in Ba/F3-p210 and K562 cells. Ba/F3-p210 and K562 cells were treated with PBS, 40 μmol/L CC or 40 μmol/L TAT-CC protein for 48 h. **a** Apoptosis analyzed by flow cytometry. Independent experiments were repeated three times. **b** Result of DNA ladder assay. TAT stands for TAT-CC. **c** Ultrastructural analysis by TEM scanning. Bar = 2 μm. **d** mRNA and protein levels of bax and bcl-2 detected by RT-PCR and western blot. TAT stands for TAT-CC

at 4 °C for 6 h with end-over-end mixing. If TAT-CC could pull-down BCR-ABL, TAT-CC and BCR-ABL can both be detected by western blot. The results show that TAT-CC could pull-down BCR-ABL protein from the lysate of Ba/F3-p210 and K562 cells (Fig. 1b; lanes 2, 5). We further performed coimmunoprecipitation assay to detect whether TAT-CC could interact with BCR-ABL protein inside cells. The result (Fig. 1b; lanes 3, 6) showed that TAT-CC could interact with BCR-ABL in Ba/F3-p210 and K562 cells.

TAT-CC fusion protein induces apoptosis in Ba/F3-p210 and K562 cells

Previously, we have demonstrated that TAT-CC protein specifically induced apoptosis in BCR-ABL positive cells, while had no effect in BCR-ABL negative cells (Huang et al. 2011). Here we further confirm the apoptotic effect of TAT-CC protein on Ba/F3-p210 and K562 cells and investigate the possible mechanism. Flow cytometry

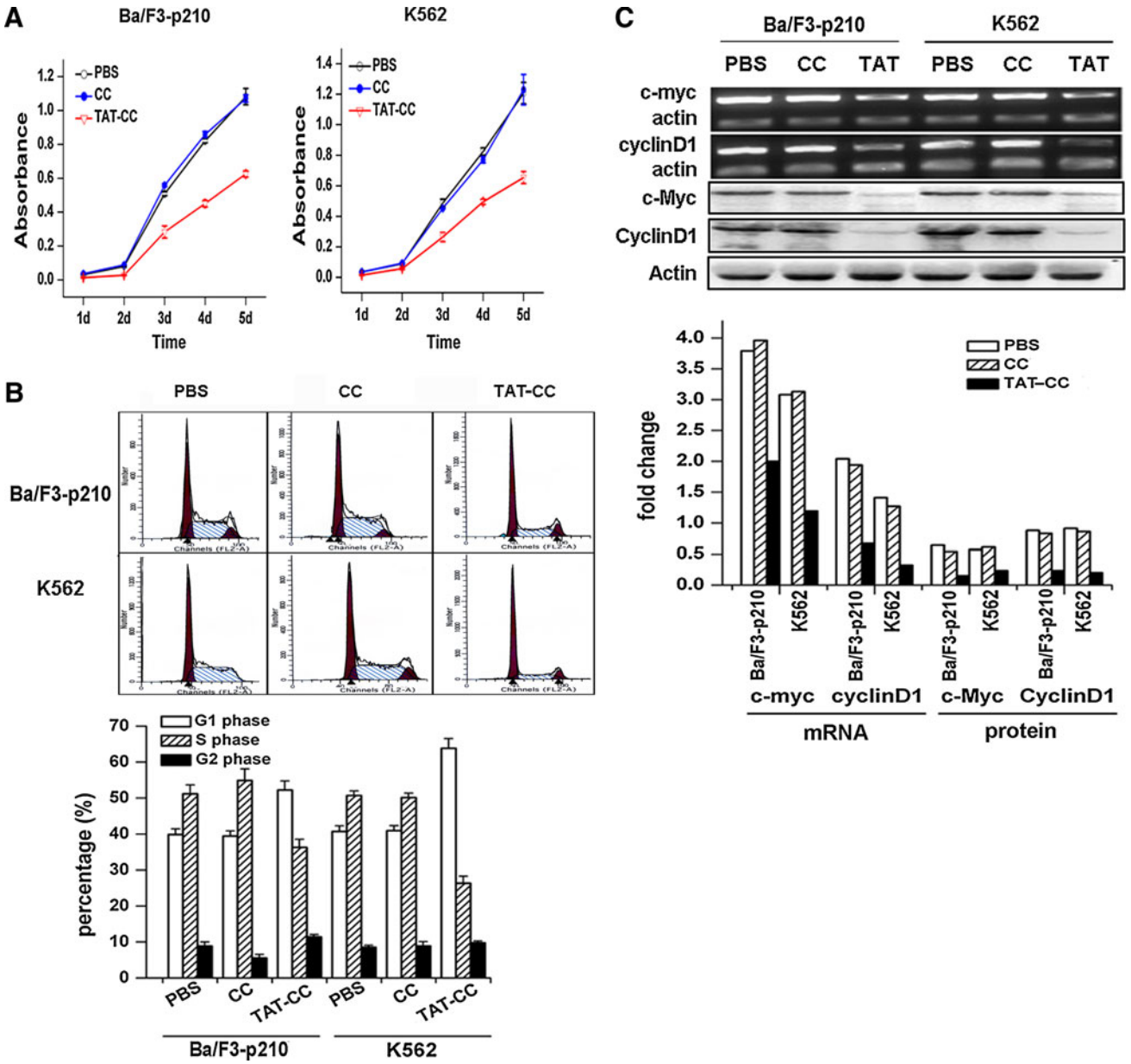

Fig. 3 TAT-CC fusion protein inhibits proliferation of Ba/F3-p210 and K562 cells. Ba/F3-p210 and K562 cells were treated with PBS, 40 μmol/L CC or 40 μmol/L TAT-CC protein for 48 h. **a** Cell growth analyzed by MTT assay. **b** Cell cycle analysis by flow cytometry. Independent experiments were repeated three times. **c** mRNA and protein levels of c-myc and cyclinD1 detected by RT-PCR and western blot. TAT is the short of TAT-CC protein

analysis (Fig. 2a) showed that TAT-CC can induce apoptosis in Ba/F3-p210 and K562 cells. The difference between the TAT-CC group and PBS group or TAT-CC group and CC group is statistically significant ($P < 0.05$), while the difference between CC group and PBS group is not significant ($P > 0.05$). To detect broken DNA fragments, we performed DNA ladder assay and the results demonstrated that obvious DNA ladders emerged in TAT-CC treated cells (Fig. 2b). Typical apoptotic bodies, nuclei with increased electronic density and widened perinuclear spaces were observed in TAT-CC treated cells (Fig. 2c). Great vacuoles, widely expanded mitochondria and lots of lysosomes were also viewed by TEM scanning (data not shown). To elucidate the possible mechanism of the apoptotic effect caused by TAT-CC, we examined the potential effect of TAT-CC on mRNA and protein levels of bax and bcl-2, which are at the mitochondrial pathway in physiological cell death. Results (Fig. 2d) suggested that the mRNA and protein levels of bax increased in TAT-CC treated cells compared to CC or PBS treated cells, while the expression of bcl-2 decreased. The expressions of bax and bcl-2 of CC treated cells were constant with PBS

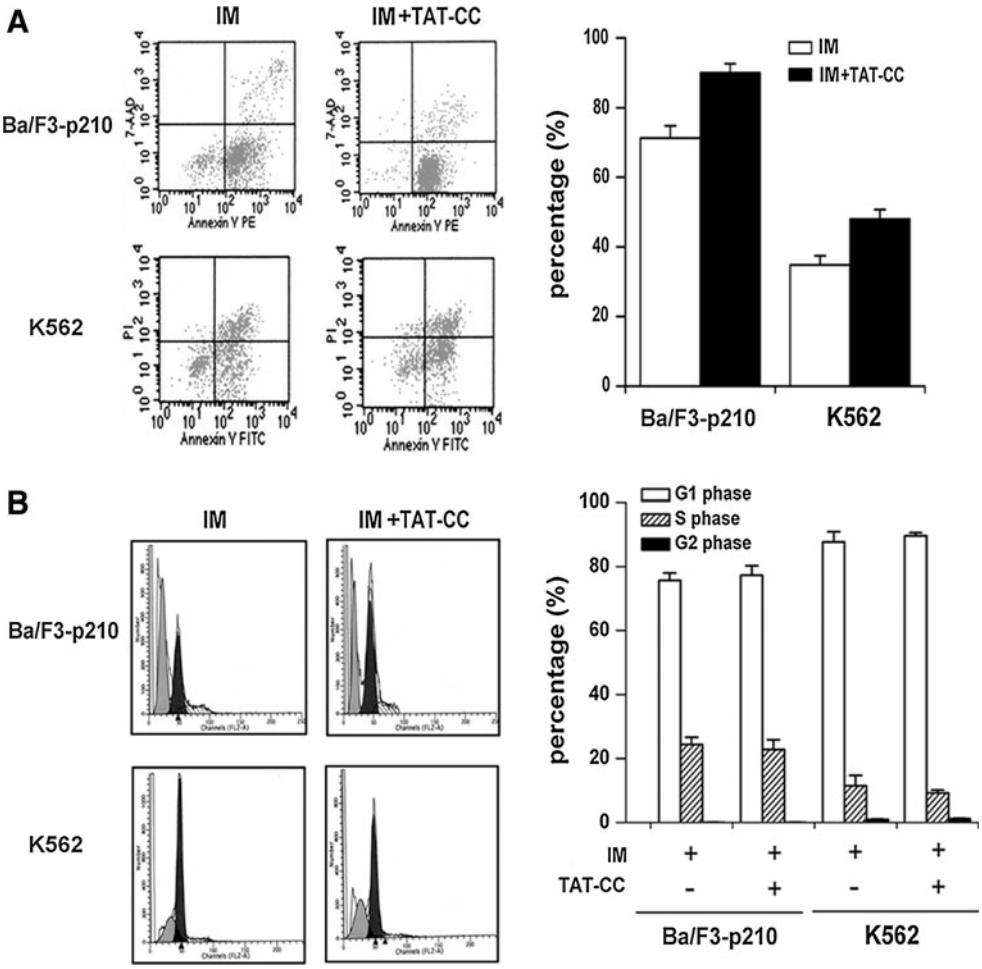

Fig. 4 TAT-CC fusion protein increases the sensitivity of Ba/F3-p210 and K562 cells to imatinib. Cell apoptosis and cell cycles were analyzed by flow cytometry. Independent experiments were repeated three times. IM stands for imatinib. **a** Results of cell apoptosis analysis. **b** Results of cell cycle analysis

treated cells. Taken together, TAT-CC can induce Ba/F3-p210 and K562 cells apoptosis and mitochondrial pathway participates in the apoptotic procedure induced by TAT-CC.

TAT-CC fusion protein blocks the proliferation of Ba/F3-p210 and K562 cells

To determine if TAT-CC had any effect on growth of Ba/F3-p210 and K562 cells, we treated cells with TAT-CC and assessed cell growth by MTT assay. Results (Fig. 3a) showed that TAT-CC inhibited the growth of Ba/F3-p210 and K562 cells. The effective inhibition was at 1st to 3rd days. The cell cycles were analyzed by flow cytometry (Fig. 3b). In TAT-CC group, the cell percentage at G1 phase increased, while S phase decreased. This demonstrated that TAT-CC prevented Ba/F3-p210 and K562 cells from G1 phase into S phase. c-Myc and CyclinD1 are two important molecules which regulate cell cycle progression. We detected the expressions of c-myc and cyclinD1 by RT-PCR and western blot (Fig. 3c). The mRNA and protein levels of c-myc and cyclinD1 was reduced by TAT-CC. Taken together, the TAT-CC can inhibit the proliferation of Ba/F3-p210 and K562 cells. c-Myc and CyclinD1 play a part in the proliferation blockage caused by TAT-CC. However, the exact mechanism remains to be further explored.

TAT-CC fusion protein increases the sensitivity of Ba/F3-p210 and K562 cells to imatinib

We were interested in if TAT-CC could enhance the effect of imatinib on BCR-ABL positive cells. Ba/F3-p210 and K562 cells were treated with imatinib alone or in combination of imatinib and TAT-CC. Cell apoptosis and cell cycles were analyzed (Fig. 4a, b). The percentages of apoptotic Ba/F3-p210 cells treated with imatinib or imatinib plus TAT-CC were 74.45 ± 1.22 and 91.49 ± 0.94, respectively, and the percentages of apoptotic K562 cells were 33.77 ± 2.5 and 48.10 ± 0.25, respectively. The increase of imatinib-mediated apoptosis is statistically significant. These results suggest that TAT-CC can enhance the apoptotic effect of imatinib on Ba/F3-p210 and K562 cells. The data of cell cycle analysis exhibited that cell cycles of each group had little differences. This indicates that TAT-CC can not reinforce the cycle arrest of imatinib on Ba/F3-p210 and K562 cells.

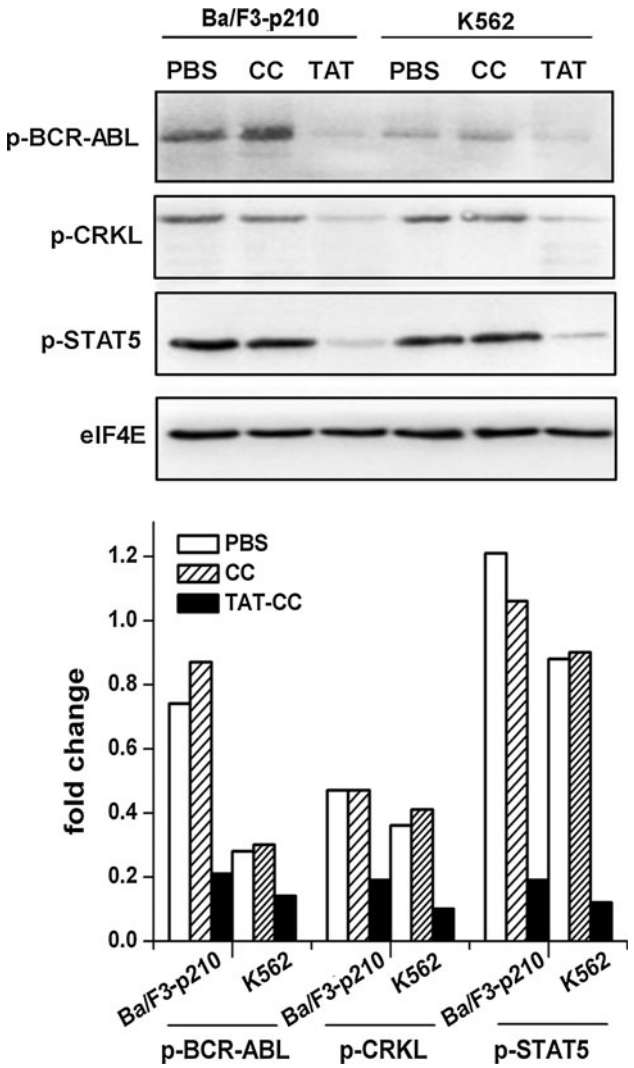

Fig. 5 TAT-CC fusion protein reduces the phosphorylation of BCR-ABL, CRKL and STAT5. Ba/F3-p210 and K562 cells were treated with PBS, 40 μmol/L CC or 40 μmol/L TAT-CC for 48 h. p-BCR-ABL, p-CRKL and p-STAT5 were analyzed by western blot with corresponding antibodies. TAT is the short of TAT-CC protein

TAT-CC fusion protein reduces the phosphorylation of BCR-ABL, CRKL and STAT5

The tetramerization of BCR-ABL is correlated to its kinase activity and transformation ability. Hence, if the tetramerization is disrupted, the phosphorylation of BCR-ABL will be reduced. STAT5 and CRKL are important downstream molecules phosphorylated by BCR-ABL (Hazlehurst et al. 2009). We analyzed the phosphorylation of BCR-ABL, CRKL and STAT5 (p-BCR-ABL, p-CRKL, p-STAT5) by western blot. The eIF4E protein was set as reference to equilibrate sample loading. The results (Fig. 5) showed that the levels of p-BCR-ABL, p-CRKL and p-STAT5 all declined in TAT-CC treated cells comparing to CC or PBS treated cells. The reduced phosphorylation of BCR-ABL indicated that TAT-CC was capable of interrupting the oligomerization of endogenous BCR-ABL.

TAT-CC fusion protein inhibits the tumorigenesis of Ba/F3-p210 cells in BALB/c mice

Our in vitro studies showed that TAT-CC reduced the phosphorylation of BCR-ABL, thus induced apoptosis and inhibited proliferation of BCR-ABL positive cells. We further explored if TAT-CC inhibited the tumorigenesis of Ba/F3-p210 cells in vivo. The syngeneic BALB/c mice serve as living incubators for the autonomous growth of Ba/F3-p210 cells. Leukemogenicity, disease latency and patterns of organ involvement which can not be assessed in vitro can be assessed in vivo. Because cells in each group were identical except for the pretreatment, differences in biological behavior can be directly attributed to the action of pretreatment. BALB/c mice were injected with TAT-CC or PBS treated Ba/F3-p210 cells. Untreated mice were set as normal control. The group of untreated mice, mice injected with PBS or TAT-CC treated cells were named as group a, b or c, respectively. From the 3rd week on, mice from group b and c began to fall ill. Ill mouse was found weight loss, hind-limb paralysis, activity reduced and hair fluffy. The experimental mice were observed for 8 months. The survival curves showed (Fig. 6a) that group c developed CML with much longer disease latency than group b and had higher survival rate. The 8 month survival rate of group b was 30 %, and group c was 70 %. The average life spans of group a, b and c were 218.1 ± 20.8, 96.2 ± 30.0 and 179.8 ± 29.3 days, respectively. TAT-CC significantly prolonged survival of group c compared to group b ($P = 0.0074$). Mice that appeared pre-morbid were killed. A normal mouse from group a was also executed as control. The representative mouse of each group was respectively named as mouse a, b or c. Peripheral blood and bone marrow were obtained and stained with Wright's dye. The liver and spleen were stained by HE staining. Wright's stain (Fig. 6b) showed that WBC increased in the peripheral blood of mouse *b* (range of WBC counts, $18.4–25.1 \times 10^6$/ml), whereas, slightly in mouse *c* (range, $8.3–12.7 \times 10^6$/ml) when compared with mouse *a* (range, $5.1–7.8 \times 10^6$/ml). Myelocytes, metagranulocytes and stab cells augmented in the bone marrow of mouse *c*, but much less than those in mouse *b*. Figure 6c showed that mouse *b* had splenomegaly. The spleen weight of group b was 0.209 ± 0.021 g, group a and c 0.114 ± 0.012 g and 0.130 ± 0.029 g, respectively. The livers of mouse *b* and *c* shrank a little. HE staining (Fig. 6d) showed that the liver structure of mouse *b* was mussy as compared with mouse *a* or *c*. Tumor cells with rod or lobulated shape infiltrated and agglomerated in the liver. A small number

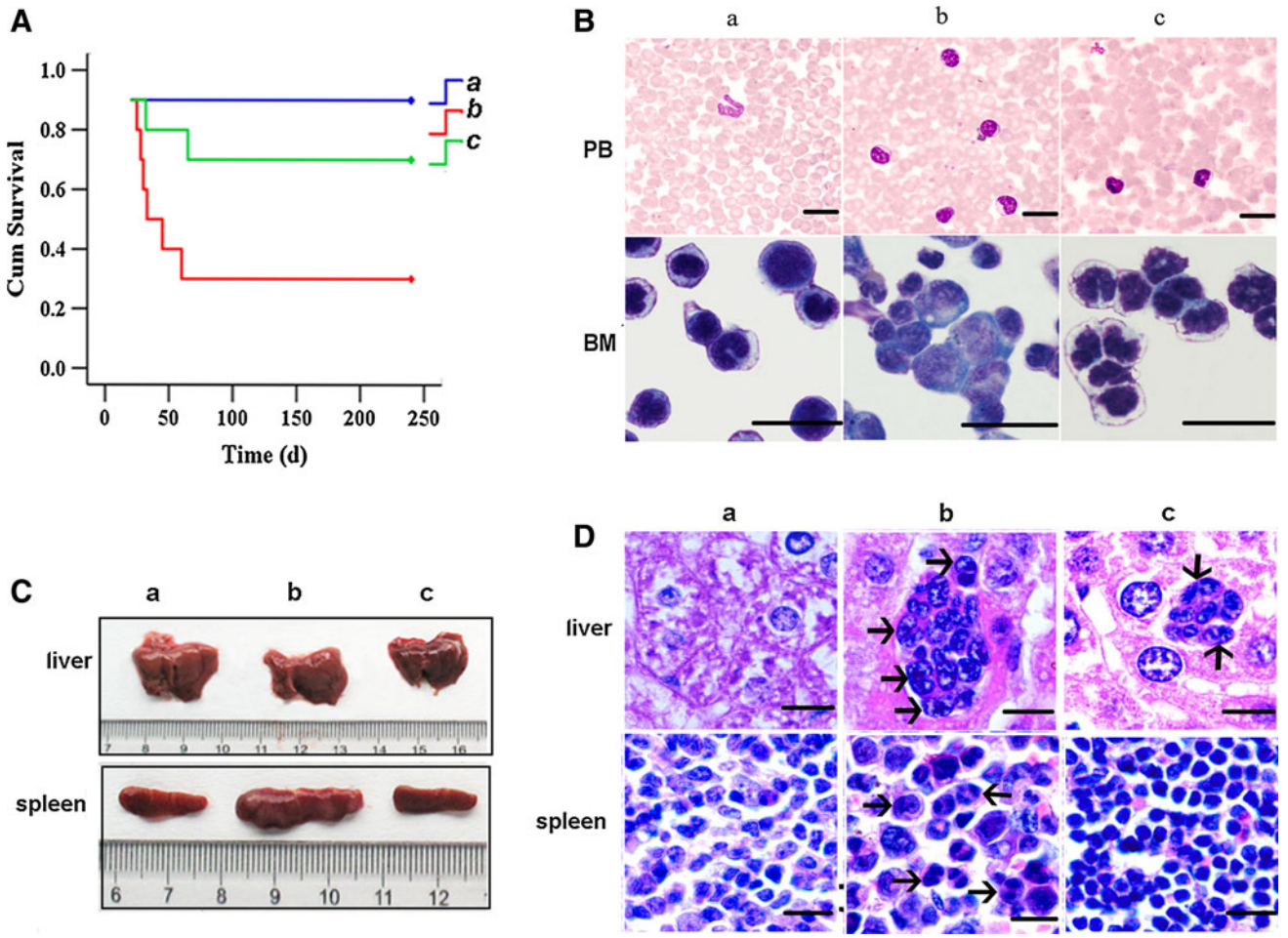

Fig. 6 TAT-CC fusion protein inhibits the tumorigenesis of Ba/F3-p210 cells in BALB/c mice. Ba/F3-p210 cells were treated with PBS or 40 μmol/L TAT-CC protein for 48 h. Cells were injected into BALB/c mice by caudal vein injection ($n = 10$). The group of untreated mice, mice injected with PBS or TAT-CC treated cells were respectively named as group a, b or c. **a** Kaplan–Meier curve. **b** Peripheral blood and bone marrow smears of group a, b, and c stained with Wright's dye. Bar = 25 μm. **c** The representive liver and spleen from group a, b, and c. **d** The liver and spleen structure of group a, b, and c mice stained with HE staining. The *arrows* indicate rod or lobulated nuclear cells. Bar = 25 μm

of tumor cells invaded into the liver of mouse *c*. The spleen organization of mouse *b* was disordered as compared with mouse *a* or *c*. Spleen nodules were completely destroyed. A large number of tumor cells with rod or lobulated nuclei infiltrated in the spleen. Spleen nodules were damaged slightly and some tumor cells invaded the spleen in mouse *c*. The tissues of heart, lung and kidney from each group did not display obvious changes (data not shown). BCR-ABL was detected in the bone marrow of mouse *b* and *c* (data not shown). These results suggested that mouse *b* and *c* had developed a CML-like disease. However, mouse *b* was much more severe than mouse *c*. Those survival mice were killed at the 8th month. The tissues from heart, liver, spleen, lung and kidney were stained with HE staining. Results showed there were no pathological changes in those organs (data not shown). This indicated that all survival mice did not develop CML-like disease.

TAT-CC fusion protein diminishes the volume of K562 subcutaneous solid tumor in nude mice

The in vitro data indicates TAT-CC induces apoptosis and inhibits proliferation in K562 cells. We wonder if it could diminish the solid tumor volume in vivo. BALB/c nude mice were subcutaneously injected with K562 cells. PBS or TAT-CC was injected into the subcutaneous solid tumor. Normal BALB/c nude mice was set as control and named as group a. PBS or TAT-CC injected mice were named as group b or c. As compared with group a or c, the tumor of group b grew much more rapidly. Mice were killed at 30th day and tumors were removed. Figure 7a shows the tumor volume curve and representive tumors from group b and c. The results indicated that TAT-CC efficiently reduced the size of the tumor. TEM scanning, TUNEL assay and immunohistochemistry were taken to detect the changes in tumor tissue. In group c, obvious apoptotic bodies and

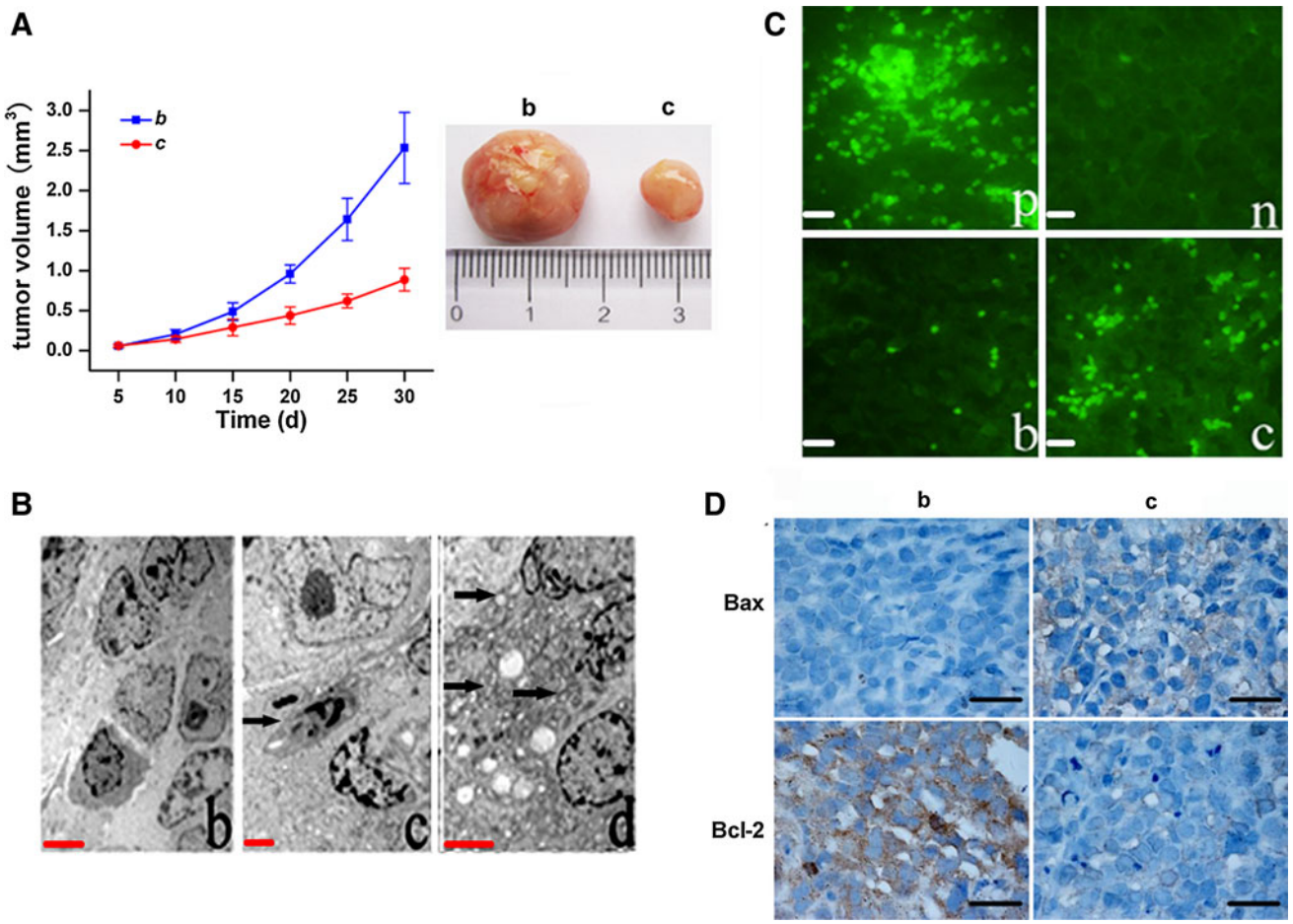

Fig. 7 TAT-CC fusion protein diminishes the volume of K562 subcutaneous solid tumor in nude mice. 1×10^7 K562 cells were subcutaneously injected into BALB/c nude mice ($n = 5$). **a** The tumor volume curve and representive tumor removed from group b or c mice at 30th day. **b** Tumor tissues analyzed by TEM scanning. *b* is the tumor tissue of group *b* mouse, bar = 5 μm; *c*, *d* is the tumor tissue of group c mouse, bar = 2 μm. The *arrows* indicate apoptotic bodies (*c*) or extensively swelling mitochondria (*d*). **c** Results of TUNEL assay. *p*,*n* represent positive and negative control, respectively. *b* is the tumor tissue of group b mouse. *c* is the tumor tissue of group c mouse. Bar = 25 μm. **d** The expression of Bax and Bcl-2 in tumor tissues of group b and c mice detected by immunohistochemistry. Bar = 25 μm

extensively swelling mitochondria were viewed by TEM scanning (Fig. 7b). We observed more broken DNA fragments in group b using TUNEL assay, which indicated that TAT-CC can induce apoptosis in K562 subcutaneous solid tumor tissue (Fig. 7c). Moreover, the expression of Bax increased while Bcl-2 decreased in group c compared with group b (Fig. 7d). In summary, TAT-CC diminishes the volume of K562 subcutaneous solid tumor in nude mice by inducing apoptosis in tumor cells.

Discussion

BCR-ABL is the cause of chronic myeloid leukemia. Both the kinase activity and oligomerization domain are crucial for BCR-ABL oncogenicity, so they may independently serve as drug targets (Zhao et al. 2002). Imatinib is a selective kinase inhibitor and has become the first choice of CML treatment (Jabbour et al. 2009). However, drug resistance and patient intolerance have become the challenges of CML therapy (Volpe et al. 2009). Targeting the BCR oligomerization domain may provide a complementary therapeutic approach to specifically disrupt BCR-ABL transformation potential.

The apoptosis in Ba/F3-p210 and K562 cells induced by TAT-CC were examined by annexinV staining, DNA ladder assay and TEM scanning. These results suggested that TAT-CC induced significantly apoptosis in Ba/F3-p210 and K562 cells. To explore the potential mechanisms, we detected the mRNA and protein levels of bax and bcl-2 which regulated apoptosis mainly via the mitochondria pathway (Rolland and Conradt 2010). Results showed that TAT-CC enhances the expression of bax and attenuates the expression of bcl-2. Thus, we concluded that mitochondrial pathway may participate in apoptosis induced by TAT-CC. However, if mitochondrial membrane permeabilization,

cytochrome c release and caspase 9 were investigated, the presumption will be more confirmable. Different effects were found between Ba/F3-p210 and K562 cells in vitro experiments. This may be caused by different genetic background of these cells. Our findings showed that TAT-CC was more effective on Ba/F3-p210 cells than on K562 cells.

The apoptotic effect caused by imatinib plus TAT-CC was nearly equal to the sum of apoptosis induced by imatinib or TAT-CC, respectively (as shown in Figs. 2a and 4a). These results suggested TAT-CC enhanced the sensitivity of Ba/F3-p210 and K562 cells to imatinib. However, TAT-CC can not boost the cell cycle blockage of imatinib. Imatinib inhibits the proliferation of the divided fraction and induces apoptosis while non-dividing cells are retained because the imatinib does not kill quiescent cells (HOLTZ and BHATIA 2004). TAT-CC may inhibit the proliferation of the divided fraction. However, the cell cycle arrest effects of imatinib and TAT-CC have no additive effect.

Furthermore, TAT-CC also reduces p-BCR-ABL, p-CRKL and p-STAT5. The BCR-ABL kinase is crucial for the development of CML. STAT5 and CRKL are important downstream molecules of BCR-ABL (Hazlehurst et al. 2009). Constitutive activation of STAT5 implicates deregulation of a transcription factor prominent in hematopoiesis. It has been reported that interference with STAT5 activation negatively affects the survival and proliferation of BCR-ABL positive cells. STAT5 activation has been implicated in CML cell apoptosis mediated by tyrosine kinase inhibitor (Shuai et al. 1996). Our study has discovered that TAT-CC down-regulated p-BCR-ABL. p-STAT5 was then suppressed by p-BCR-ABL down-regulation. Thus, the survival and proliferation of BCR-ABL positive cells were inhibited. CRKL is a significant signaling protein to the development of Ph+ leukemia (Sattler and Salgia 1998). The phosphorylation status of CRKL has been identified as a surrogate marker of BCR-ABL tyrosine kinase activity (Oda et al. 1994). Our results showed the level of p-CRKL correlated with the level of p-BCR-ABL.

We examined the effect of TAT-CC on Ba/F3-p210 leukemogenesis in mice and found it increased the life span by an average of 101.1 days. Because mice have a maximal life span of around 36 months, this represents a very marked elongation in life expectancy. There were three mice still alive, which were injected with Ba/F3-p210 cells. Tissue examinations showed the three mice did not develop CML-like disease. This was mainly due to the limitation of the model methodology. We investigated the treatment effect of TAT-CC on K562 subcutaneous solid tumor in mice and found it inhibited tumor expansion and reduced tumor volume. Cell apoptosis induced by TAT-CC via mitochondria pathway was one of the effective factors, which was consistent with in vitro experiments.

Taken together, our results suggested that targeting the BCR CC domain may provide a complementary therapeutic strategy to inhibit BCR-ABL oncogenicity. The combination of oligomerization interruption and tyrosine kinase inhibitor provides a prospective approach for CML treatment.

Acknowledgments This work was supported by the National Natural Science Foundation of China No. 30670901 to Wenli Feng.

References

Baccarani M, Rosti G, Castagnetti F et al (2009) Comparison of imatinib 400 mg and 800 mg daily in the front-line treatment of high-risk, Philadelphia-positive chronic myeloid leukemia: a European LeukemiaNet Study. Blood 113:4497–4504

Beissert T, Puccetti E, Bianchini A, Guller S, Boehrer S, Hoelzer D, Ottmann OG, Nervi C, Ruthardt M (2003) Targeting of the N-terminal coiled coil oligomerization interface of BCR interferes with the transformation potential of BCR-ABL and increases sensitivity to STI571. Blood 102:2985–2993

Beissert T, Hundertmark A, Kaburova V, Travaglini L, Mian AA, Nervi C, Ruthardt M (2008) Targeting of the N-terminal coiled coil oligomerization interface by a helix-2 peptide inhibits unmutated and imatinib-resistant BCR/ABL. Int J Cancer 122:2744–2752

de Lavallade H, Apperley JF, Khorashad JS, Milojkovic D, Reid AG, Bua M, Szydlo R, Olavarria E, Kaeda J, Goldman JM, Marin D (2008) Imatinib for Newly Diagnosed Patients With Chronic Myeloid Leukemia: incidence of Sustained Responses in an intention-to-treat analysis. J Clin Oncol 26:3358–3363

Deininger MWN, Goldman JM, Melo JV (2000) The molecular biology of chronic myeloid leukemia. Blood 96:3343–3356

Deininger M, Buchdunger E, Druker BJ (2005) The development of imatinib as a therapeutic agent for chronic myeloid leukemia. Blood 105:2640–2653

Druker BJ, Guilhot F, O'Brien SG et al (2006) Five-year follow-up of patients receiving imatinib for chronic myeloid leukemia. N Engl J Med 355:2408–2417

Faderl S, Talpaz M, Estrov Z, O'Brien S, Kurzrock R, Kantarjian HM (1999) The biology of chronic myeloid leukemia. N Engl J Med 341:164–172

Frankel AD, Pabo CO (1988) Cellular uptake of the tat protein from human immunodeficiency virus. Cell 55:1189–1193

Gao Y, Xiong D, Yang M et al (2004) Efficient inhibition of multidrug-resistant human tumors with a recombinant bispecific anti-P-glycoprotein [times] anti-CD3 diabody. Leukemia 18:513–520

Ghaffari S, Wu H, Gerlach M, Han Y, Lodish HF, Daley GQ (1999) BCR-ABL and v-SRC tyrosine kinase oncoproteins support normal erythroid development in erythropoietin receptor-deficient progenitor cells. Proc Natl Acad Sci USA 96:13186–13190

Green M, Loewenstein PM (1988) Autonomous functional domains of chemically synthesized human immunodeficiency virus tat trans-activator protein. Cell 55:1179–1188

Hazlehurst LA, Bewry NN, Nair RR, Pinilla-Ibarz J (2009) Signaling networks associated with BCR-ABL–Dependent transformation. Cancer Control 16:100–107

Herce HD, Garcia AE (2007) Molecular dynamics simulations suggest a mechanism for translocation of the HIV-1 TAT peptide across lipid membranes. Proc Natl Acad Sci 104:20805–20810

Holtz MS, Bhatia R (2004) Effect of imatinib mesylate on chronic myelogenous leukemia hematopoietic progenitor cells. Leuk Lymphoma 45:237–245

Huang Z, Ji M, Peng Z, Huang S, Xiao Q, Li C, Zeng J, Gao M, Feng W (2011) Purification of TAT-CC-HA protein under native condition, and its transduction analysis and biological effects on BCR-ABL positive cells. Biomed Pharmacother 65:183–192

Ilaria RJ, Van Etten R (1995) The SH2 domain of P210BCR/ABL is not required for the transformation of hematopoietic factor-dependent cells. Blood 86:3897–3904

Jabbour E, Kantarjian HM, Jones D et al (2009) Imatinib mesylate dose escalation is associated with durable responses in patients with chronic myeloid leukemia after cytogenetic failure on standard-dose imatinib therapy. Blood 113:2154–2160

Jacquel A, Herrant M, Defamie V et al (2005) A survey of the signaling pathways involved in megakaryocytic differentiation of the human K562 leukemia cell line by molecular and c-DNA array analysis. Oncogene 25:781–794

Kinyanjui MW, Fixman ED (2008) Cell-penetrating peptides and proteins: new inhibitors of allergic airways disease. This review is an invited paper from 2007 ICRH Leadership in Science: a forum for trainees and new investigators. Can J Physiol Pharmacol 86:1–7

Klein E, Vánky F, Ben-Bassat H, Neumann H, Ralph P, Zeuthen J, Polliack A (1976) Properties of the K562 cell line, derived from a patient with chronic myeloid leukemia. Int J Cancer 18:421–431

Lugo T, Pendergast A, Muller A, Witte O (1990) Tyrosine kinase activity and transformation potency of BCR-ABL oncogene products. Science 247:1079–1082

Martin S, James DG (2003) Molecular mechanisms of transformation by the BCR-ABL oncogene. Semin Hematol 40:4–10

McWhirter JR, Galasso DL, Wang JY (1993) A coiled-coil oligomerization domain of BCR is essential for the transforming function of BCR-ABL oncoproteins. Mol Cell Biol 13:7587–7595

Melo JV, Deininger MW (2004) Biology of chronic myelogenous leukemia–signaling pathways of initiation and transformation. Hematol Oncol Clin North Am 18:545–568 (vii–viii)

Mian AA, Oancea C, Zhao Z, Ottmann OG, Ruthardt M (2009) Oligomerization inhibition, combined with allosteric inhibition, abrogates the transformation potential of T315I-positive BCR/ABL. Leukemia 23:2242–2247

Oda T, Heaney C, Hagopian JR, Okuda K, Griffin JD, Druker BJ (1994) Crkl is the major tyrosine-phosphorylated protein in neutrophils from patients with chronic myelogenous leukemia. J Biol Chem 269:22925–22928

Palandri F, Iacobucci I, Castagnetti F et al (2008) Front-line treatment of Philadelphia positive chronic myeloid leukemia with imatinib and interferon-{alpha}: 5-year outcome. Haematologica 93:770–774

Rapoport M, Lorberboum-Galski H (2009) TAT-based drug delivery system—new directions in protein delivery for new hopes? Expert Opin Drug Deliv 6:453–463

Richard JP, Melikov K, Vives E, Ramos C, Verbeure B, Gait MJ, Chernomordik LV, Lebleu B (2003) Cell-penetrating peptides. A reevaluation of the mechanism of cellular uptake. J Biol Chem 278:585–590

Rolland SG, Conradt B (2010) New role of the BCL2 family of proteins in the regulation of mitochondrial dynamics. Curr Opin Cell Biol 22:852–858

Sattler M, Salgia R (1998) Role of the adapter protein CRKL in signal transduction of normal hematopoietic and BCR/ABL-transformed cells. Leukemia 12:637–644

Schroering AG, Kothandapani A, Patrick SM, Kaliyaperumal S, Sharma VP, Williams KJ (2009) Prolonged cell cycle response of HeLa cells to low-level alkylation exposure. Cancer Res 69:6307–6314

Shuai K, Halpern J, ten Hoeve J, Rao X, Sawyers C (1996) Constitutive activation of STAT5 by the BCR-ABL oncogene in chronic myelogenous leukemia. Oncogene 13:247–254

Strecker A, Salzberger U, Mayer J (1993) Specimen preparation for transmission electron microscopy (TEM)–reliable method for cross sections and brittle materials. Prakt Metallogr 30:482–495

Tzoracoleftherakis E, Sdralis E, Maroulis J, Ravazoula P (2010) Radiofrequency ablation in breast cancer. Cancer Res 69:2106

Vive‘s E, Brodin P, Lebleu B (1997) A truncated HIV-1 Tat protein basic domain rapidly translocates through the plasma membrane and accumulates in the cell nucleus. J Biol Chem 272:16010–16017

Volpe G, Panuzzo C, Ulisciani S, Cilloni D (2009) Imatinib resistance in CML. Cancer Lett 274:1–9

Zhang X, Subrahmanyam R, Wong R, Gross AW, Ren R (2001) The NH2-terminal coiled-coil domain and tyrosine 177 play important roles in induction of a myeloproliferative disease in mice by BCR-ABL. Mol Cell Biol 21:840–853

Zhao X, Ghaffari S, Lodish H, Malashkevich VN, Kim PS (2002) Structure of the BCR-ABL oncoprotein oligomerization domain. Nat Struct Mol Biol 9:117–120